Proceeding Series of the Brazilian Society of Computational and Applied Mathematics, v. 11, n. 1, 2025.

Trabalho apresentado no XLIII CNMAC, Centro de Convenções do Armação Resort - Porto de Galinhas - PE, 2024

Proceeding Series of the Brazilian Society of Computational and Applied Mathematics

Computational Simulation of a Low Mach Number Turbulent Reacting Flow

Jonatan Ismael Eisermann[1], Álvaro Luiz de Bortoli[2]
Federal University of Rio Grande do Sul, Porto Alegre, RS

Abstract. This work presents a computational approach for low Mach number turbulent reacting flows employing Large Eddy Simulation (LES). In this perspective, a mathematical model based on equations of continuity, momentum, mixture fraction and temperature is deduced and used to obtain numerical solutions for the Sandia DME D diffusion flame on a three-dimensional computational mesh. The model is discretized on the mesh using the Finite Difference method, and then solved using the Improved Euler method. This approach makes it possible to simulate low Mach number turbulent reacting flows efficiently and robustly.

Keywords. Low Mach number, turbulent reacting flow, diffusion flame, Large Eddy Simulation, Finite Difference method, Improved Euler method

1 Introduction

Low Mach number flows, characterized by velocities significantly lower than the speed of sound, present specific challenges in computational fluid dynamics, particularly concerning turbulent flows. Unlike high-speed flows where compressibility effects dominate, the behavior of low Mach number flows is primarily governed by viscous forces and, when applicable, turbulence, due to the minimal influence of compressibility. This distinction enables the utilization of specific computational methods to accurately model and simulate turbulent flows in such regimes.

To deal with the complexities of low Mach number turbulent flows, researchers often turn to the Large Eddy Simulation (LES) methodology [11]. LES resolves the larger turbulent structures explicitly while modeling the effects of smaller scales, making it computationally efficient compared to Direct Numerical Simulation (DNS), which resolves all turbulent scales. By focusing computational resources on the most energetic turbulent motions, LES strikes a balance between accuracy and computational cost, making it suitable for simulating turbulent flows.

In this study, we present a computational approach based on the LES methodology adapted specifically for low Mach number turbulent reacting flows. Our method aims to provide a comprehensive understanding of turbulent phenomena while maintaining computational efficiency. Furthermore, we apply this approach to simulate a co-flow relative to the Sandia DME D turbulent diffusion flame [12]. Through our simulations, we aim to improve understanding of low Mach number turbulent flows and their interaction with diffusion flames, contributing to advances in combustion research and engineering applications.

[1]jonatan.eisermann@ufrgs.br
[2]dbortoli@mat.ufrgs.br

2 Mathematical model

Reactive flows can be modeled using incompressible, low Mach number and compressible formulations. In the incompressible formulation, the fluid density remains constant, which limits its ability to take into account flow changes due to heat release. In the low Mach number formulation, suitable for subsonic flows, acoustic waves are neglected and the density varies with temperature but remains constant with respect to pressure. On the other hand, compressible formulation captures the effects of heat release and pressure variations, making it more suitable for high-speed flows where compressibility effects are significant. However, in numerical simulations, it often requires smaller time integration steps due to the consideration of acoustic waves.

The basic fluid dynamics equations used to model incompressible, low Mach number and compressible flows cover the conservation of mass, momentum and energy/enthalpy. When dealing with reactive flows it is also necessary to include the mass fraction equation of each chemical species involved or, in the specific case of diffusion flames, the mixture fraction equation. This equation is particularly attractive because by obtaining the mixture fraction it is possible to obtain, at low computational cost, reasonable approximations for the temperature using the Burke-Schumann analytical solution [3].

2.1 Primitive variables formulation

Assuming the appropriate differentiability conditions for the variables involved in the flow, the aforementioned equations are presented in the following subsections using Einstein's summation notation [7]. Thus, for example, in a three-dimensional space $\mathbf{x} = (x_1, x_2, x_3)$ with velocity vector denoted by $\mathbf{u} = (u_1, u_2, u_3)$, where the component u_i corresponds to the velocity along the x_i-direction, $i = 1, 2, 3$, the summation

$$\sum_{j=1}^{3} \frac{\partial u_i}{\partial x_j} \tag{1}$$

is compactly denoted by $\frac{\partial u_i}{\partial x_j}$, where i represents the free index, and j and k are dummy indices.

2.1.1 Continuity equation

In fluid dynamics, the continuity equation is based on the principle of conservation of the total mass involved in a closed system. It describes the changes in the density of the fluid, ρ, for a fixed point, caused by variations in the velocity vector $\mathbf{u}$ over time t, being described by the expression

$$\frac{\partial \rho}{\partial t} + \frac{\partial (\rho u_j)}{\partial x_j} = 0. \tag{2}$$

2.1.2 Momentum equation

The conservation of momentum is based on Newton's Second Law, which states that the rate of change of momentum over time is equal to the forces applied on the system. These forces primarily include the pressure p, dynamic viscosity μ and gravity g. In our study, we will consider a Newtonian fluid and neglect the effect of gravity, so the momentum equation considered is

$$\frac{\partial (\rho u_i)}{\partial t} + \frac{\partial (\rho u_i u_j)}{\partial x_j} = -\frac{\partial p}{\partial x_i} + \frac{\partial}{\partial x_j}\left[\mu\left(\frac{\partial u_i}{\partial x_j} + \frac{\partial u_j}{\partial x_i} - \frac{2}{3}\delta_{ij}\frac{\partial u_k}{\partial x_k}\right)\right], \qquad i = 1, 2, 3, \tag{3}$$

where δ_{ij} denotes the Kronecker delta ($\delta_{ij} = 1$, if $i = j$; $\delta_{ij} = 0$, if $i \neq j$).

2.1.3 Mixture fraction and temperature equations

In diffusion flames, the mixture fraction (Z) is a quantity used to measure the proportion of one component (usually the fuel) within a mixture originating from two distinct feed streams: one containing the fuel and the other containing the oxidant. The mathematical expression that governs the mixture fraction can be derived from the equations that describe the mass fractions of the chemical species [6], and it can be represented by

$$\frac{\partial(\rho Z)}{\partial t} + \frac{\partial(\rho u_j Z)}{\partial x_j} = \frac{\partial}{\partial x_j}\left(\frac{\mu}{\mathrm{Sc}}\frac{\partial Z}{\partial x_j}\right), \tag{4}$$

where Sc denotes the Schmidt number of the flow.

From the calculation of Z in (4), we can obtain reasonable approximations for the temperature through the analytical Burke-Schumann solution for diffusion flames. Based on this approach, for a fuel stream with temperature T_1 and an oxidant stream with temperature T_2, the temperature, in Kelvin, of the mixture can be approximated by the function $T : [0,1] \to \mathbb{R}_+$ expressed by

$$T(Z) = \begin{cases} T_2 + (T_1 - T_2)Z + \left(\frac{QY_{\mathrm{F},1}}{c_p \nu_{\mathrm{F}} \mathrm{W}_{\mathrm{F}}}\right) Z, & \text{if } Z \le Z_{\mathrm{st}} \\ T_2 + (T_1 - T_2)Z + \left(\frac{QY_{\mathrm{O}_2,2}}{c_p \nu_{\mathrm{O}_2} \mathrm{W}_{\mathrm{O}_2}}\right)(1 - Z), & \text{otherwise} \end{cases}, \tag{5}$$

where Z_{st} is the stoichiometric value of Z, $Y_{\mathrm{F},1}$ is the mass fraction of fuel in the fuel stream, $Y_{\mathrm{O}_2,2}$ is the mass fraction of O_2 in the oxidizing stream, Q is the heat of combustion, c_p is the specific heat capacity, ν_{F} and ν_{O_2} are, respectively, the stoichiometric coefficient of the fuel and O_2, and W_{F} and $\mathrm{W}_{\mathrm{O}_2}$ denote, respectively, the molecular weight of the fuel and O_2.

2.2 Favre averaged formulation

In the LES approach, Favre averaging or density-weighted averaging [8] is utilized on certain compressible flow variables to separate turbulent fluctuations from the mean flow. This filtering process leads to a simplified representation of the nonlinear convective terms within the governing equations compared to the traditional Reynolds averaging [10]. In the Favre decomposition some dependent variables Φ involved in the governing equations are decomposed into an average component $\widetilde{\Phi}$ and a fluctuation component Φ'', such that

$$\Phi = \widetilde{\Phi} + \Phi'', \qquad \overline{\rho\Phi''} = 0, \tag{6}$$

where $\overline{(\cdot)}$ denotes the Reynolds average. In this context, the following properties are valid:

$$\overline{\rho\,\Phi} = \overline{\rho}\widetilde{\Phi}, \qquad \overline{\rho\Phi''} = 0, \qquad \overline{\rho\,\widetilde{\Phi}} = \overline{\rho}\widetilde{\Phi}. \tag{7}$$

2.2.1 Continuity equation

Using the Reynolds average in the continuity equation (2), we have

$$\overline{\frac{\partial \rho}{\partial t} + \frac{\partial(\rho u_j)}{\partial x_j}} = \overline{0}. \tag{8}$$

Decomposing the variable u_j from the above equation as done in (6), we obtain

$$0 = \overline{\frac{\partial \rho}{\partial t}} + \overline{\frac{\partial(\rho u_j)}{\partial x_j}} = \frac{\partial \overline{\rho}}{\partial t} + \frac{\partial(\overline{\rho(\widetilde{u}_j + u_j'')})}{\partial x_j} = \frac{\partial \overline{\rho}}{\partial t} + \frac{\partial(\overline{\rho\widetilde{u}_j + \rho u_j''})}{\partial x_j} = \frac{\partial \overline{\rho}}{\partial t} + \frac{\partial(\overline{\rho\widetilde{u}_j} + \overline{\rho u_j''})}{\partial x_j}. \tag{9}$$

From this and the properties (7), we summarize the continuity equation to

$$\frac{\partial \overline{\rho}}{\partial t} + \frac{\partial(\overline{\rho}\widetilde{u}_j)}{\partial x_j} = 0. \tag{10}$$

DOI: 10.5540/03.2025.011.01.0366

2.2.2 Momentum equation

Using the Reynolds average in the momentum equation (3), it follows that

$$\overline{\frac{\partial(\rho u_i)}{\partial t} + \frac{\partial(\rho u_i u_j)}{\partial x_j}} = \overline{-\frac{\partial p}{\partial x_i} + \frac{\partial}{\partial x_j}\left[\mu\left(\frac{\partial u_i}{\partial x_j} + \frac{\partial u_j}{\partial x_i} - \frac{2}{3}\delta_{ij}\frac{\partial u_k}{\partial x_k}\right)\right]} \tag{11}$$

$$\overline{\frac{\partial(\rho u_i)}{\partial t}} + \overline{\frac{\partial(\rho u_i u_j)}{\partial x_j}} = \overline{-\frac{\partial p}{\partial x_i}} + \overline{\frac{\partial}{\partial x_j}\left[\mu\left(\frac{\partial u_i}{\partial x_j} + \frac{\partial u_j}{\partial x_i} - \frac{2}{3}\delta_{ij}\frac{\partial u_k}{\partial x_k}\right)\right]} \tag{12}$$

$$\underbrace{\overline{\frac{\partial(\rho u_i)}{\partial t}}}_{(i)} + \underbrace{\overline{\frac{\partial(\rho u_i u_j)}{\partial x_j}}}_{(ii)} = -\frac{\partial \overline{p}}{\partial x_i} + \frac{\partial}{\partial x_j}\underbrace{\overline{\left[\mu\left(\frac{\partial u_i}{\partial x_j} + \frac{\partial u_j}{\partial x_i} - \frac{2}{3}\delta_{ij}\frac{\partial u_k}{\partial x_k}\right)\right]}}_{(iii)}. \tag{13}$$

Note that:

(i)
$$\overline{\frac{\partial(\rho u_i)}{\partial t}} = \overline{\frac{\partial(\rho(\tilde{u}_i + u_i''))}{\partial t}} = \overline{\frac{\partial(\rho\tilde{u}_i + \rho u_i'')}{\partial t}} = \frac{\partial(\overline{\rho\tilde{u}_i} + \overline{\rho u_i''})}{\partial t} = \frac{\partial(\overline{\rho}\tilde{u}_i)}{\partial t}; \tag{14}$$

(ii)
$$\overline{\frac{\partial(\rho u_i u_j)}{\partial x_j}} = \frac{\partial\overline{[\rho(\tilde{u}_i + u_i'')(\tilde{u}_j + u_j'')]}}{\partial x_j} \tag{15}$$

$$= \frac{\partial(\overline{\rho\tilde{u}_i\tilde{u}_j + \rho\tilde{u}_i u_j'' + \rho u_i''\tilde{u}_j + \rho u_i'' u_j''})}{\partial x_j} \tag{16}$$

$$= \frac{\partial(\overline{\rho\tilde{u}_i\tilde{u}_j} + \overline{\rho\tilde{u}_i u_j''} + \overline{\rho u_i''\tilde{u}_j} + \overline{\rho u_i'' u_j''})}{\partial x_j} \tag{17}$$

$$= \frac{\partial(\overline{\rho}\tilde{u}_i\tilde{u}_j + (\overline{\rho u_j''})\tilde{u}_i + (\overline{\rho u_i''})\tilde{u}_j + \widetilde{\overline{\rho}u_i'' u_j''})}{\partial x_j} \tag{18}$$

$$= \frac{\partial(\overline{\rho}\tilde{u}_i\tilde{u}_j + \widetilde{\overline{\rho}u_i'' u_j''})}{\partial x_j} \tag{19}$$

$$= \frac{\partial(\overline{\rho}\tilde{u}_i\tilde{u}_j)}{\partial x_j} + \frac{\partial(\widetilde{\overline{\rho}u_i'' u_j''})}{\partial x_j}; \tag{20}$$

(iii)
$$\overline{\mu\left(\frac{\partial u_i}{\partial x_j} + \frac{\partial u_j}{\partial x_i} - \frac{2}{3}\delta_{ij}\frac{\partial u_k}{\partial x_k}\right)} = \overline{\mu}\left(\frac{\partial\tilde{u}_i}{\partial x_j} + \frac{\partial\tilde{u}_j}{\partial x_i} - \frac{2}{3}\delta_{ij}\frac{\partial\tilde{u}_k}{\partial x_k}\right). \tag{21}$$

Thus, it follows from (13) that, for $i = 1, 2, 3$,

$$\frac{\partial(\overline{\rho}\tilde{u}_i)}{\partial t} + \frac{\partial(\overline{\rho}\tilde{u}_i\tilde{u}_j)}{\partial x_j} = -\frac{\partial\overline{p}}{\partial x_i} + \frac{\partial}{\partial x_j}\left[\overline{\mu}\left(\frac{\partial\tilde{u}_i}{\partial x_j} + \frac{\partial\tilde{u}_j}{\partial x_i} - \frac{2}{3}\delta_{ij}\frac{\partial\tilde{u}_k}{\partial x_k}\right) - \widetilde{\overline{\rho}u_i'' u_j''}\right]. \tag{22}$$

To solve the above equations through LES, it is necessary to express the Reynolds stresses $\widetilde{\overline{\rho}u_i'' u_j''}$ in relation to the average flow components. According to Boussinesq's hypothesis [1], turbulent stresses are linked to average velocity gradients in a way similar to the way viscous stresses are related to instantaneous velocity gradients, such that

$$-\widetilde{\overline{\rho}u_i'' u_j''} = \mu_t\left(\frac{\partial\tilde{u}_i}{\partial x_j} + \frac{\partial\tilde{u}_j}{\partial x_i} - \frac{2}{3}\delta_{ij}\frac{\partial\tilde{u}_k}{\partial x_k}\right). \tag{23}$$

The artificial viscosity μ_t controls the strength of flow diffusion and needs to be modeled appropriately for the equation's numerical resolution procedures. On a computational mesh with filter size Δ the Smagorinsky model for μ_t is given by

$$\mu_t = \overline{\rho}(C\Delta)^2\sqrt{2\tilde{S}_{ij}\tilde{S}_{ij}}, \qquad \tilde{S}_{ij} = \frac{1}{2}\left(\frac{\partial \tilde{u}_i}{\partial x_j} + \frac{\partial \tilde{u}_j}{\partial x_i}\right), \tag{24}$$

with C denoting a constant coefficient.

2.2.3 Mixture fraction and temperature equations

Following a similar procedure to that performed in items (i) and (ii) of the previous subsection, but now substituting u_i by Z, we obtain for the mixture fraction equation:

$$\frac{\partial(\overline{\rho}\tilde{Z})}{\partial t} + \frac{\partial(\overline{\rho}\tilde{u}_j\tilde{Z})}{\partial x_j} = \frac{\partial}{\partial x_j}\left(\frac{\overline{\mu}}{\mathrm{Sc}}\frac{\partial \tilde{Z}}{\partial x_j} - \overline{\rho}\widetilde{u_j''Z}\right). \tag{25}$$

Here, we consider

$$-\overline{\rho}\widetilde{u_j''Z} = \frac{\mu_t}{\mathrm{Sc}}\frac{\partial \tilde{Z}}{\partial x_j}. \tag{26}$$

The formulation for the temperature function remains the same as equation (5), just considering $\tilde{Z}$ instead of Z. This formulation, together with equations (10), (22) and (25) form the mathematical model that will be used in the next section for the large eddy simulation of a low Mach number turbulent reacting flow. Furthermore, a dimensionless version of the equations can be consulted in Appendix D of Calegari's work [5].

3 Numerical results

The analysis and validation of a mathematical model are achieved through appropriate numerical resolution. In this context, using the model developed in the previous section, a simulation of a low Mach number turbulent flow was implemented in Matlab software[1], version R2024a, and conducted on a computer equipped with an Intel Core i7-8550U processor (1.8 GHz, Turbo Boost up to 4.0 GHz, with 4 cores). More specifically, we focus on the Sandia DME D diffusion flame within the Sydney piloted burner configuration [12].

In the Sandia DME D flame, the aforementioned burner, featuring three coaxial jets, generates a turbulent diffusion flame where a fuel composed of 20% dimethyl ether and 80% air is injected from a central tube with diameter $d = 7.45$ mm. Flame stabilization is achieved through a pilot annulus, with internal and external diameters of 8 mm and 18.2 mm, respectively. For combustion to occur, an air co-flow of 25.4 cm $\times$ 25.4 cm is injected under ambient conditions, surrounding the pilot jet. The corresponding Reynolds number for this flame is 29,300.

The numerical resolution of the mathematical model for the Sandia DME D flame, previously developed, requires us to discretize the domain in order to transform the real solution of the model into a discrete function defined at a limited number of points in space. In this context, we employ a computational mesh comprising $121 \times 71 \times 71$ points along the x, y, and z (x_1, x_2, and x_3) directions, respectively, covering the Sydney piloted burner with dimensions $40d \times 7d \times 7d$. Furthermore, the discretization of the model on the mesh is done using the fourth order Finite Difference method [2].

[1] `https://www.mathworks.com/products/matlab.html`.

For the initial conditions of the problem, all mesh points were set to ambient temperature and pressure. Furthermore, at the points corresponding to the main jet nozzle (fuel inlet), the variables were set as follows: $\tilde{u}_1 = 45.9$ m/s, $\tilde{u}_2 = \tilde{u}_3 = 0$ m/s, $\tilde{Z} = 1$, $\overline{\rho} = 1.323$ kg/m^3, and $\overline{\mu} = 10^{-5}$ Pa·s. At the points corresponding to the pilot and the air inlet, the variables were set as $\tilde{u}_1 = 1$ m/s, $\tilde{u}_2 = \tilde{u}_3 = 0$ m/s, $\tilde{Z} = 0$, $\overline{\rho} = 1.184$ kg/m^3, and $\overline{\mu} = 10^{-5}$ Pa·s. These conditions were extended to the remaining points, except for the velocity $\tilde{u}_1$, which is considered null. Conversely, for the boundary conditions, the fluid inlet boundary was defined identically to the initial conditions. For the remaining system boundaries, Neumann conditions with a zero normal derivative were applied by mirroring the variable values from the adjacent interior point at each boundary point.

Based on the initial and boundary conditions, the model is then solved through an iterative process using the Improved Euler method [4] with time step $h = 10^{-6}$ s. To address the coupling between pressure and velocity present in the the equations, the Semi-Implicit Method for Pressure-Linked Equations (SIMPLE) is adopted. Although it was originally proposed for incompressible flows, this method has been extended to solve compressible flows with low Mach number [9].

On average, the simulation took around eight minutes for every thousand iterations performed on the computer used. Illustrating the flame formation, some numerical results for velocity, mixture fraction and temperature along the central plane of the burner can be seen in Figure 1.

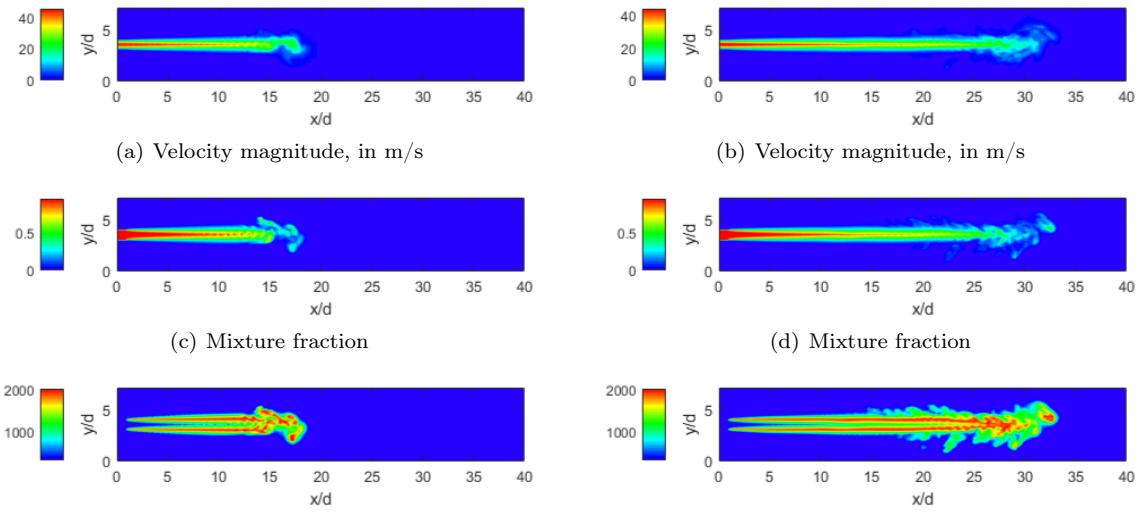

(a) Velocity magnitude, in m/s

(b) Velocity magnitude, in m/s

(c) Mixture fraction

(d) Mixture fraction

(e) Temperature, in Kelvin

(f) Temperature, in Kelvin

Figure 1: Numerical results in iterations 10,000 (left) and 25,000 (right). Source: the authors.

From the numerical results obtained and summarized in the (sub)figures above, we observe that the simulated flame structure starts with a potential zone spanning approximately ten diameters d in length, which transitions into a turbulent plume at its end. In this context, although the simulation of the initial part of the flame may be comparatively simpler, numerically efficient and robust techniques are imperative to accurately capture the turbulence present in the intermediate and final parts of the flame.

4 Final considerations

The mathematical model employed in this study has shown its adequacy for low Mach number turbulent reacting flows, although it is based on simplifying assumptions for temperature calcula-

DOI: 10.5540/03.2025.011.01.0366

tions. By filtering out the smallest length scales present in the governing equations, LES combined with an effective computational method for solving flow equations has emerged as a viable, efficient and robust approach to simulating such complex systems.

As part of our ongoing research, we are currently comparing numerical data with experimental data of the studied flame, adding chemical species concentration equations to the mathematical model, optimizing model parameter selection, quantifying simulation errors, and developing a stability analysis of the Sandia DME D flame.

Acknowledgments

The first author of this work thanks the financial support from the National Council for Scientific and Technological Development (CNPq) - Brazil, under grant 141504/2021-8. Prof. De Bortoli thanks the CNPq - Brazil for the financial support under grant 309271/2021-5.

References

[1] J. Boussinesq. **Théorie analytique de la chaleur: mise en harmonie avec la thermodynamique et avec la théorie mécanique de la lumière**. Vol. 2. Gauthier-Villars, 1903.

[2] R. L. Burden, J. D. Faires, and A. M. Burden. **Numerical Analysis**. 10th ed. Boston: Cengage Learning, 2015. ISBN: 978-1-305-25366-7.

[3] S. P. Burke and T. E. W. Schumann. "Diffusion Flames". In: **Indust. Eng. Chem.** 20 (1928), pp. 998–1004. DOI: 10.1021/ie50226a005.

[4] J. C. Butcher. **The Numerical Analysis of Ordinary Differential Equations: Runge-Kutta and General Linear Methods**. Chichester: John Wiley and Sons, 1987.

[5] P. C. Calegari. "Simulação computacional de escoamentos reativos com baixo número de Mach aplicando técnicas de refinamento adaptativo de malhas". PhD thesis. USP, 2012.

[6] A. L. De Bortoli, G. S. L. Andreis, and F. N. Pereira. **Modeling and Simulation of Reactive Flows**. Amsterdam - Netherlands: Elsevier, 2015. ISBN: 978-0-12-802974-9.

[7] A. Einstein. "Die Grundlage der allgemeinen Relativitäistheorie". In: **Annalen der Physik** 49.7 (1916), pp. 769–822. DOI: 10.1002/andp.19163540702.

[8] A. Favre. "The equations of compressible turbulent gases". In: **Annual Summary Report AD0622097** (1965).

[9] C. R. Maliska. **Transferência de Calor e Mecânica dos Fluídos Computacional**. 2nd ed. Rio de Janeiro: LTC, 2004. ISBN: 978-8521613961.

[10] N. Peters. **Turbulent Combustion**. Cambridge: Cambridge University Press, 2000. ISBN: 0-521-66082-3.

[11] J. Smagorinsky. "General Circulation Experiments with the Primitive Equations: The Basic Experiment". In: **Monthly Weather Review** 91.3 (1963), pp. 99–164. DOI: 10.1175/1520-0493(1963)091<0099:GCEWTP>2.3.CO;2.

[12] TNF Workshop. **Piloted DME (dimethyl ether) Jet Flames**. Online. Accessed March 11, 2024. URL: https://tnfworkshop.org/data-archives/pilotedjet/piloteddme/.

